Visible-to-UV triplet-triplet annihilation upconversion from a thermally activated delayed fluorescence/pyrene pair in an air-saturated solution

Hak-Lae Lee*, Myung-Soo Lee*, Hyun Park**, Won-Sik Han***, and Jae-Hyuk Kim*,†

*Department of Chemical and Environmental Engineering, Pusan National University, Busan 46241, Korea
**Naval Architecture & Ocean Engineering, Pusan National University, Busan 46241, Korea
***Department of Chemistry, Seoul Women's University, Seoul 01797, Korea

Abstract−Despite increasing use of triplet-triplet annihilation upconversion (TTA-UC) of low-energy visible light, the generation of ultraviolet (UV) photons by TTA remains challenging because of the difficulty in finding sensitizers and acceptors with suitable energy levels. Here, we report efficient, photostable visible-to-UV TTA-UC in an air-saturated solution using a new pair with suitable energy levels: a thermally activated delayed fluorescence (TADF) molecule and pyrene. 4CzIPN, which has extremely small energy difference ΔE_{ST} (0.083 eV), was used as the TADF sensitizer to promote effective triplet energy transfer to the acceptor. When oleic acid was used as an effective singlet oxygen receptor in an air-saturated solution, the 4CzIPN/pyrene pair exhibited bright upconverted emission at 370-430 nm under 445 nm laser excitation, but no noticeable upconverted emission was observed when 4CzIPN was paired with previously reported UV-emitting acceptors [2,5-diphenyloxazole (PPO), *p*-terphenyl, and *p*-quaterphenyl]. TTA was confirmed by the quadratic dependence of the upconverted emission intensity on the 445 nm laser power density. The maximum quantum yield of the upconverted emission from the 4CzIPN/pyrene pair was 0.66%, which is considerable when compared with that of a previously reported visible-to-UV TTA-UC system with a biacetyl/PPO pair (0.58%).

Keywords: Upconversion, Triplet-Triplet Annihilation, Anti-Stokes Emission, UV Generation, Thermally Activated Delayed Fluorescence

INTRODUCTION

Ultraviolet (UV) radiation continues to emerge as an essential tool in environmental applications, including degradation of environmental contaminants [1], photocatalysis [2], and water disinfection [3]. Because the UV wavelengths in sunlight are blocked by the atmosphere, electricity-powered UV lamps are used for environmental application to water or air. A material that effectively converts long-wavelength solar energy into short-wavelength UV radiation without electricity would facilitate widespread use of solar UV radiation in these environmental applications. Furthermore, much effort has been made to harness solar energy and convert it into usable forms (i.e., electricity and resources such as hydrogen) for many years. However, most solar-based technologies exhibit poor light-harvesting efficiency owing to their inherent limitations; photons with energies below the band gap or highest occupied molecular orbital-lowest unoccupied molecular orbital gap energy of their materials cannot be harvested [4]. Photon upconversion (UC), a photochemical process in which a high-energy photon can be generated by combining two or more low-energy photons, has the potential to make better use of a large fraction of this wasted energy. Two types of UC mechanisms are usually considered, those based on lanthanide ions and on triplet-triplet annihilation (TTA)

[5-8]. The lanthanide-ion-based UC process reportedly has limited solar applications because it requires high incident light intensities ($\sim 10^4$ W cm^{-2}) and has poor efficiency [9]. On the other hand, TTA-based upconversion (TTA-UC) can be achieved even under realistically weak excitation intensities of 1-10 mW cm^{-2} and is known to have quite high efficiency of 3-40%, which makes this UC approach attractive for widespread adoption in solar devices [10-13]. TTA-UC is a bimolecular process that involves a sensitizer and an acceptor. The sensitizer absorbs low-energy photons into its triplet excited state by intersystem crossing (ISC) and then transfers the energy to the acceptor through triplet-triplet energy transfer (TTET). Two excited acceptors then undergo TTA to produce upconverted emission of a single high-energy photon [14]. TTA-UC typically requires an organic chromophore pair, that is, a sensitizer and an acceptor, that satisfies the following energy criteria: the S_1 energy of the sensitizer should be lower than that of the acceptor, whereas the T_1 energy of the sensitizer should be higher than that of the acceptor [15,16]. Because the sensitizers that have typically been employed in TTA-UC have a relatively large energy difference (ΔE_{ST}) between the S_1 and T_1 states, the range of available acceptors suitable for a particular sensitizer has been very limited [17-20]. Furthermore, a sensitizer with a large ΔE_{ST} has an excited triplet state with lower energy, resulting in less energy shifting. Therefore, only a few studies have successfully demonstrated noticeable visible-to-UV TTA-UC using typical sensitizers and UV-emitting acceptors [21,22].

Wu et al. showed recently that a thermally activated delayed fluorescence (TADF) molecule, which is capable of ISC in the absence

†To whom correspondence should be addressed.
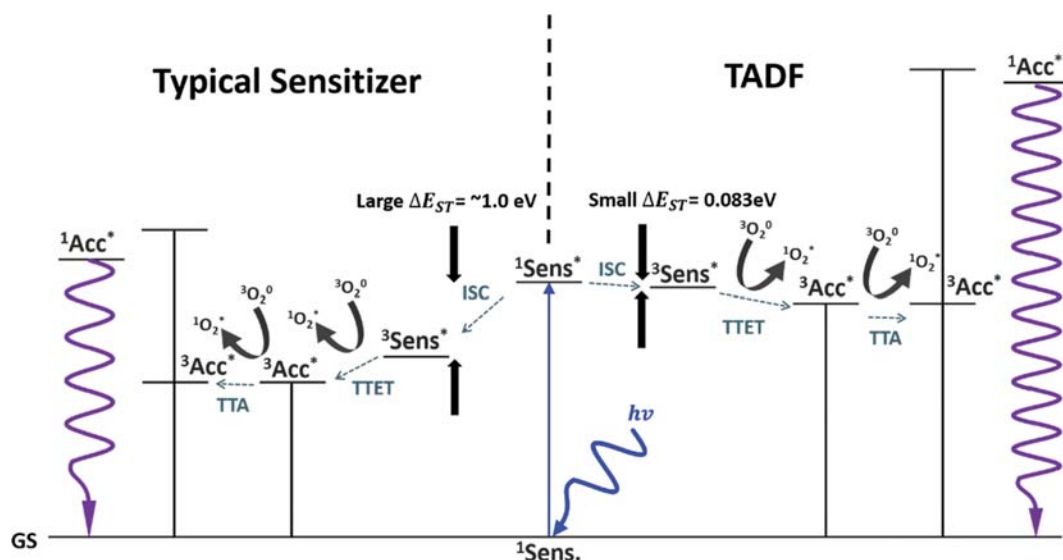E-mail: jaehyuk.kim@pusan.ac.kr

Fig. 1. Schematic Jablonski diagram of the photochemical processes of TTA-UC using typical sensitizers (left) and TADF sensitizers (right).

of heavy metal atoms, can be employed as a sensitizer in a TTA-UC system [23]. Unlike conventional organic sensitizer molecules having an S_1 energy that is much higher than the T_1 energy (~1.0 eV), TADF molecules have an extremely small energy difference between the S_1 and T_1 states (~100 meV) [24]. That is, carefully designed TADF molecules can effectively produce higher-energy triplet excitons and thus enable efficient TTA-UC with larger energy shifts (Fig. 1). They successfully demonstrated a solid-state green-to-blue TTA-UC system with an energy shift of 0.73 eV by employing the red TADF molecule 4CzTPN-Ph as a sensitizer and 9,10-diphenylanthracene as an acceptor. More recently, Yanai et al. demonstrated how to maximize the anti-Stokes shift in visible-to-UV TTA-UC systems by matching the energy levels of the TADF sensitizers and appropriate UV-emitting acceptors [25]. By employing a prototypical TADF molecule based on carbazolyl dicyanobenzene, 4CzIPN, as a sensitizer, they obtained visible-to-UV TTA-UC with a significantly larger energy shift (0.82 eV). However, their experiments were conducted in a deoxygenated organic solvent to prevent oxygen quenching, which greatly limits further practical applications.

In this work, we report photochemically stable upconverted UV emission from a new pair consisting of a TADF molecule as a sensitizer and pyrene as an acceptor, which is realized in an air-saturated solution for the first time. 4CzIPN, with T_1=2.37 eV and S_1= 2.46 eV [26], was selected as the TADF sensitizer. To obtain a photostable visible-to-UV TTA-UC system, oleic acid (OA) was used as a singlet oxygen receptor in an air-saturated solution because it is well known to consume generated singlet oxygen; thus, it protects the sensitizer from oxidation and maintains high TTA-UC stability even under oxygen-rich conditions [27]. The TTA-UC performance of a 4CzIPN/pyrene solution was evaluated and compared with that of UC pairs containing three previously reported UV-emitting acceptors, 2,5-diphenyloxazole (PPO), *p*-terphenyl (TP), and *p*-quaterphenyl (QP) [25,28], in the presence and absence of OA in the solution phase. All of the experimental data presented

below are consistent with the production of upconverted UV emission from the 4CzIPN/pyrene pair by TTA. In addition, the results clearly indicate that the upconverted UV emission from the 4CzIPN/pyrene pair is remarkably high and photostable even under an air-saturated condition when OA is included as a singlet oxygen receptor, whereas no noticeable upconverted emission is observed when 4CzIPN is paired with PPO, TP, or QP.

MATERIALS AND METHODS

1. Materials

4CzIPN was synthesized according to the literature [24,29]. The UV-emitting acceptors (pyrene, PPO, TP, and QP), Coumarin 6, and OA were purchased from Aldrich. All solvents and reagents were used as received unless otherwise stated.

Chromophore stock solutions were prepared by dissolving an appropriate amount of the solute in tetrahydrofuran (THF). The final concentrations of the stock solutions of 4CzIPN, pyrene, PPO, TP, and QP were 1.3, 16.5, 15, 43.4, and 32.6 mM, respectively. Although 4CzIPN, pyrene, PPO, and TP dissolved well in THF, QP did not, owing to its low solubility [25]. All the stock solutions were stored in the dark before use. Each TTA-UC solution was prepared by adding an aliquot of the stock solution to 2 ml of THF. The final concentrations of pyrene, PPO, TP, and QP in the TTA-UC solutions were 0.66, 1.81, 17.4, and 2.61 mM, respectively, whereas the 4CzIPN concentration was fixed at 50.7 mM in all the samples. The photostability of TTA-UC solutions with OA contents of 0-10 vol% was tested. The TTA-UC solutions without OA were degassed by N_2 purging for 10 min and sealed by para films before spectroscopic measurement.

2. Photoluminescence Measurements

Static absorption and Stokes emission spectra were acquired and analyzed using a spectrofluorometer (FS5-MCS, Edinburgh Instruments, UK). Anti-Stokes emission spectra were acquired using a custom laser setup, in which UC samples were excited at an angle
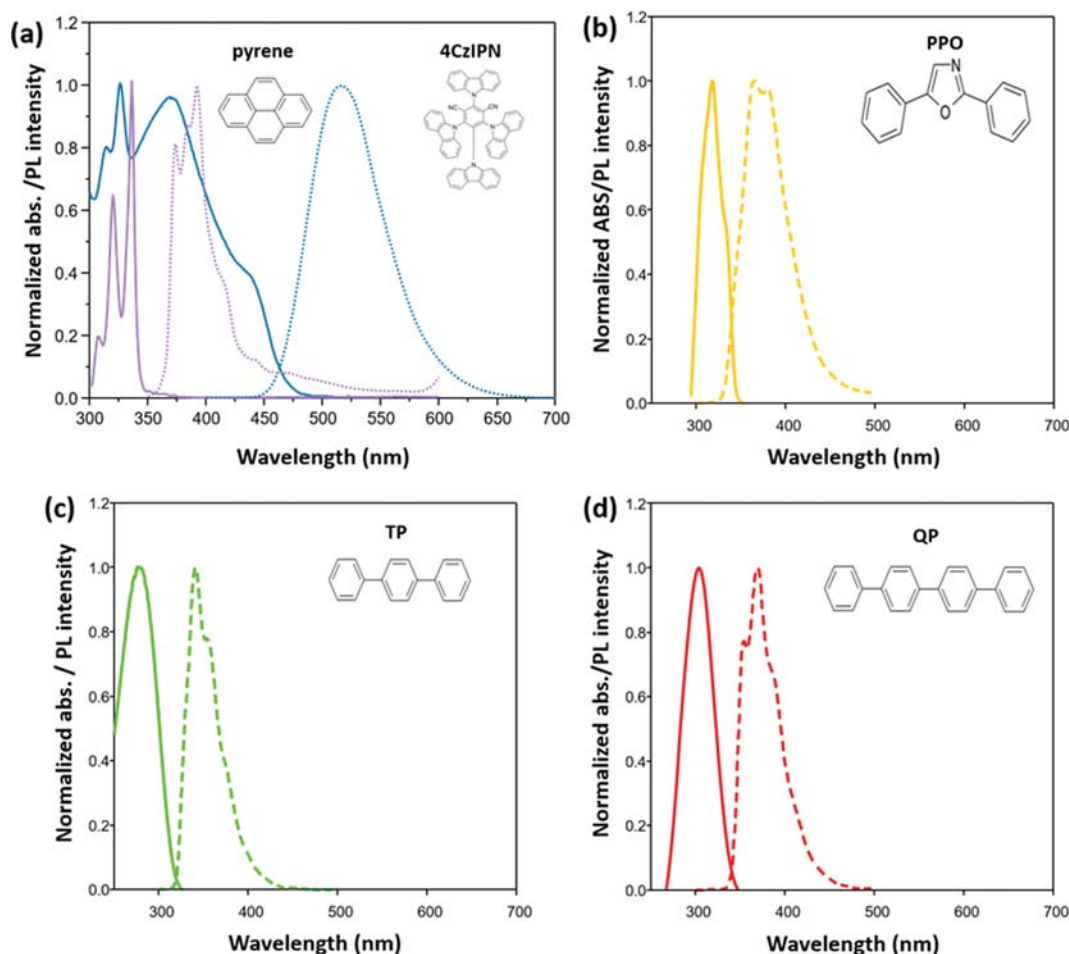
Fig. 2. Molecular structures and normalized absorption (solid) and emission (dashed) spectra of (a) 4CzIPN (blue) and pyrene (purple), (b) PPO, (c) TP, and (d) QP in THF.

of approximately 90° by a 445 nm commercial diode laser. The emission was modulated by an optical chopper (80 Hz) and directed to a monochromator (Oriel Cornerstone, Newport Corporation, USA) using a series of focusing lenses; scattered laser light was removed using a 425 nm short-pass filter. The signal was then detected using an Oriel photomultiplier tube and processed by a lock-in amplifier (SRB10 DSP, Stanford Research Systems, USA). The incident laser intensity was adjusted using a continuously variable neutral density filter and measured using a power meter (843-R, Newport Corporation, USA). The photostability of the UC samples was measured by recording the UC emission intensity at the 394, 364, 344, and 370 nm peaks corresponding to pyrene, PPO, TP, and QP, respectively, in time-interval scanning mode for 100 min.

The TTA-UC efficiency (ϕ_{UC}) was determined using Eq. (1) [30], where ϕ, A, I, and η represent the quantum yield, absorbance, integrated fluorescence intensity, and refractive index of the solvent, respectively.

$$\phi_{UC} = 2\phi_{std}\left(\frac{A_{std}}{A_{UC}}\right)\left(\frac{I_{UC}}{I_{std}}\right)\left(\frac{\eta_{UC}}{\eta_{std}}\right)^2 \tag{1}$$

The subscript "std" indicates a standard sample used as a quan-

tum counter (Coumarin 6 was used as the standard, $\phi_{std}=88.2\%$), and "UC" denotes the UC sample.

RESULTS AND DISCUSSION

1. Photoluminescence Characterizations of Chromophores

Fig. 2 shows the absorption and emission spectra of 4CzIPN, pyrene, PPO, TP, and QP in THF. A broad absorption band of 4CzIPN appears from 300 to 500 nm, whereas pyrene shows three characteristic absorption peaks between 300 and 350 nm. The emission spectrum of pyrene shows the most intense band around 390 nm and a less intense shoulder near 470 nm. The emission peaks of PPO, TP, and QP are centered at 364, 344, and 370 nm, respectively. An excitation wavelength of 445 nm was chosen to selectively excite 4CzIPN because it is sufficiently distant from the absorption bands of pyrene, PPO, TP, and QP. In the TTA-UC process, increasing the acceptor concentration generally results in stronger UC emission owing to efficient bimolecular energy transfer by TTET and TTA. However, in a TTA-UC system employing pyrene as an acceptor, the pyrene concentration needs to be optimized because excess pyrene causes an undesirable increase in excimer formation, which limits the UC emission. In this work, the opti-
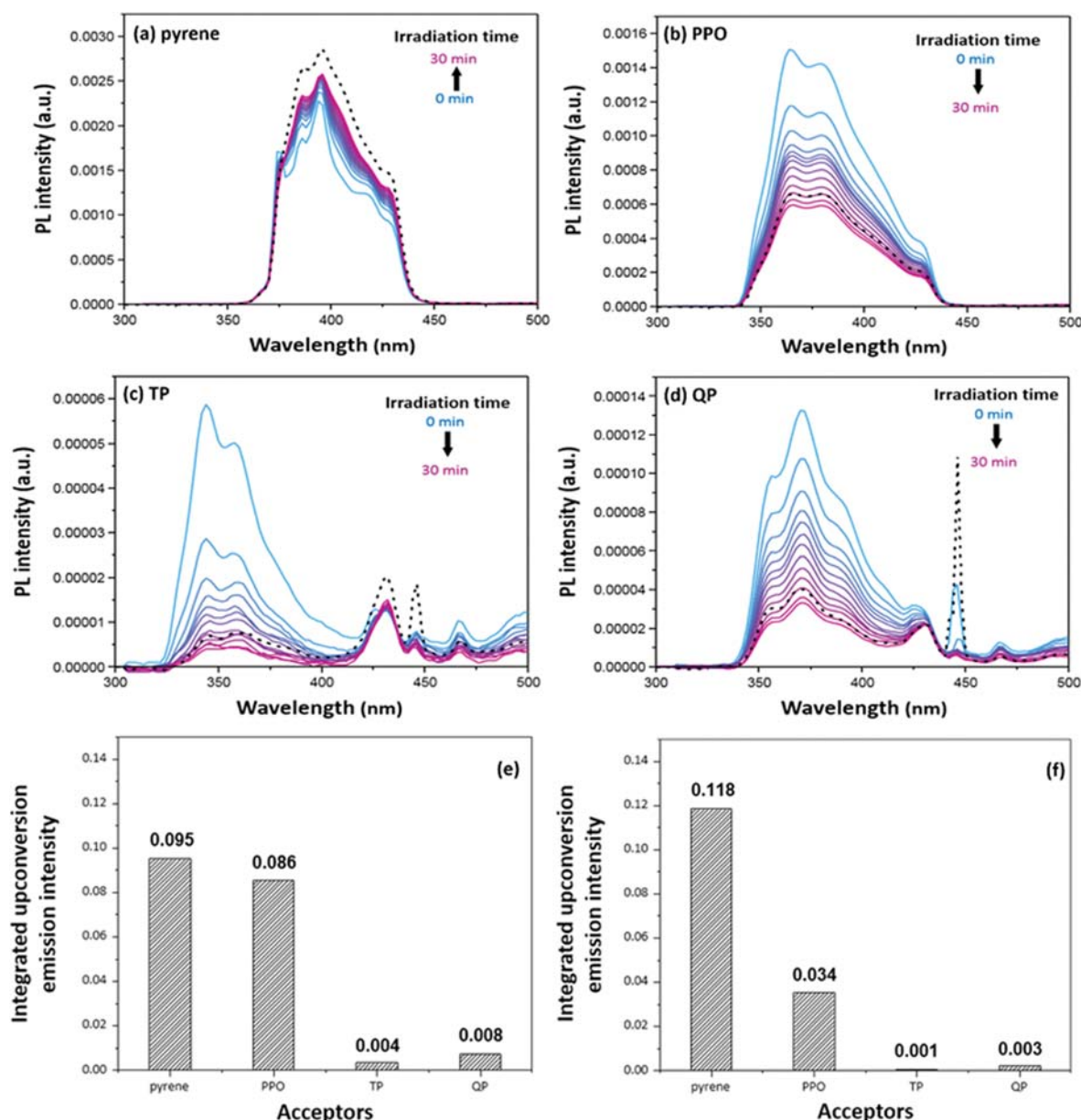
Fig. 3. UC emission spectra of (a) 4CzIPN/pyrene, (b) 4CzIPN/PPO, (c) 4CzIPN/TP, and (d) 4CzIPN/QP in degassed THF under 445 nm laser excitation for various durations. The dotted lines in (a)-(d) show the UC emission spectra of samples that were re-degassed after 30 min of 445 nm laser excitation. Integrated UC emission spectra of four UC pairs (e) at beginning of laser exposure and (f) after 30 min of exposure to 445 nm laser.

mal concentrations of 4CzIPN and pyrene were determined to be 50.7 and 660 μM, respectively.

2. TTA-UC Spectra

Fig. 3(a)-(d) show the time-course UC spectra of degassed THF solutions containing various acceptors (pyrene, PPO, TP, and QP) along with 4CzIPN under selective laser excitation at 445 nm. Both the 4CzIPN/pyrene (Fig. 3(a)) and 4CzIPN/PPO (Fig. 3(b)) pairs displayed intense upconverted emission between 350 and 450 nm in the degassed THF solution. Further, as previously reported in the literature [25], the degassed THF solutions containing 4CzIPN/ TP (Fig. 3(c)) and 4CzIPN/QP (Fig. 3(d)) showed upconverted emission between 340 and 400 nm, which corresponds to the UVA

region. When the upconverted spectra of the samples were recorded under continuous 445 nm laser irradiation, the 4CzIPN/pyrene pair showed a slight increase in UC intensity, whereas the 4CzIPN/ PPO, 4CzIPN/TP, and 4CzIPN/QP pairs exhibited a rapid decrease in UC intensity during 30 min of exposure time, indicating poor photostability. Fig. 3(e) and (f) show the integrated UC emission intensity at the beginning of laser irradiation and after 30 min of irradiation, respectively. Specifically, the initial value of the integrated UC emission intensity of the 4CzIPN/pyrene pair was 29-times higher than that of the 4CzIPN/TP solution, and the integrated UC emission intensity of 4CzIPN/pyrene after 30 min of irradiation was almost 35-times higher than that of the 4CzIPN/

PPO pair. The rapid disappearance of UC emission over time can be caused by either photobleaching of 4CzIPN or oxygen quenching of the triplet excited sensitizer in solution during the measurement [31]. To further investigate the effect of oxygen quenching, the samples were re-degassed with N_2 gas after 30 min of UC intensity measurement. Only the re-degassed THF solution containing the 4CzIPN/pyrene pair exhibited slightly increased upconverted emission after re-degassing, whereas no noticeable upconverted emission was observed from the samples containing the 4CzIPN/PPO, 4CzIPN/TP, and 4CzIPN/QP pairs (dotted lines in Fig. 3(a)-(d)), indicating that rapid photobleaching of 4CzIPN is the main reason for the UC intensity decrease when it is paired with PPO, TP, and QP. These results clearly indicate that the 4CzIPN/pyrene pair supports relatively photo-stable visible-to-UV TTA-UC better than the other chromophore pairs in highly diffusive solutions, which can be ascribed to effective intermolecular interactions between 4CzIPN and pyrene.

To determine whether the upconverted emission could be observed in a mixed solution of OA/THF, in which diffusive interactions between the sensitizers and acceptors are relatively prohibited [32], the UC intensities of the UC pairs in the OA/THF mixture were measured under identical measurement conditions but without the deoxygenation step. In our previous paper, we reported that a mixture of polyisobutylene and hexadecane can serve as an effective medium for TTA-UC under atmospheric conditions [33]. In addition, Liu et al. showed that the reducing ability of soybean oil enables it to consume the singlet oxygen generated in the TTET process, which consequently enables TTA-UC even in the presence of oxygen [34]. In the present experiment, we added OA, which is the main component of soybean oil, to the medium to eliminate the need for deoxygenation. Fig. 4(a) and (b) show the normalized UC spectra of the UC pairs in a deaerated solution and in an OA/THF (10 vol% OA) mixture, respectively. UC emission from the 4CzIPN/TP and 4CzIPN/QP pairs in the OA/THF mixture was not observed even at an excitation intensity of 6,000 mW cm^{-2}. Weak upconverted emission of the 4CzIPN/PPO pair in the OA/THF mixture was detected between 400 and 500 nm, but it was not obvious and appeared with considerable noise, as shown in Fig. 4(b). In contrast, the 4CzIPN/pyrene pair clearly exhibited upconverted UV emission in the 350-440 nm range even in the air-saturated mixture of OA/THF. This significant UC emission from the 4CzIPN/pyrene pair in the OA/THF medium demonstrates that the sensitizer/acceptor pair of 4CzIPN/pyrene can serve as an excellent chromophore couple for realizing visible-to-UV TTA-UC even in an environment with limited diffusion. Considering that the anti-Stokes shift is also important for quantitative TTA-UC analysis, we calculated the energy shifts between 4CzIPN and the four acceptors on the basis of our experiment data, as presented in Fig. 4(c). Theoretically, the largest anti-Stokes shift of 0.82 eV is obtainable from the acceptor TP, which is enabled by the use of a TADF sensitizer having an extremely small ΔE_{ST} value. Although the relatively small anti-Stokes shift of pyrene (0.44 eV) is lower than that of the other UV-emitting acceptors previously reported by other researchers, our results indicate that the sensitizer/acceptor pair of 4CzIPN/pyrene shows promise for realizing the highest achievable UC efficiency between 350 and 440 nm.
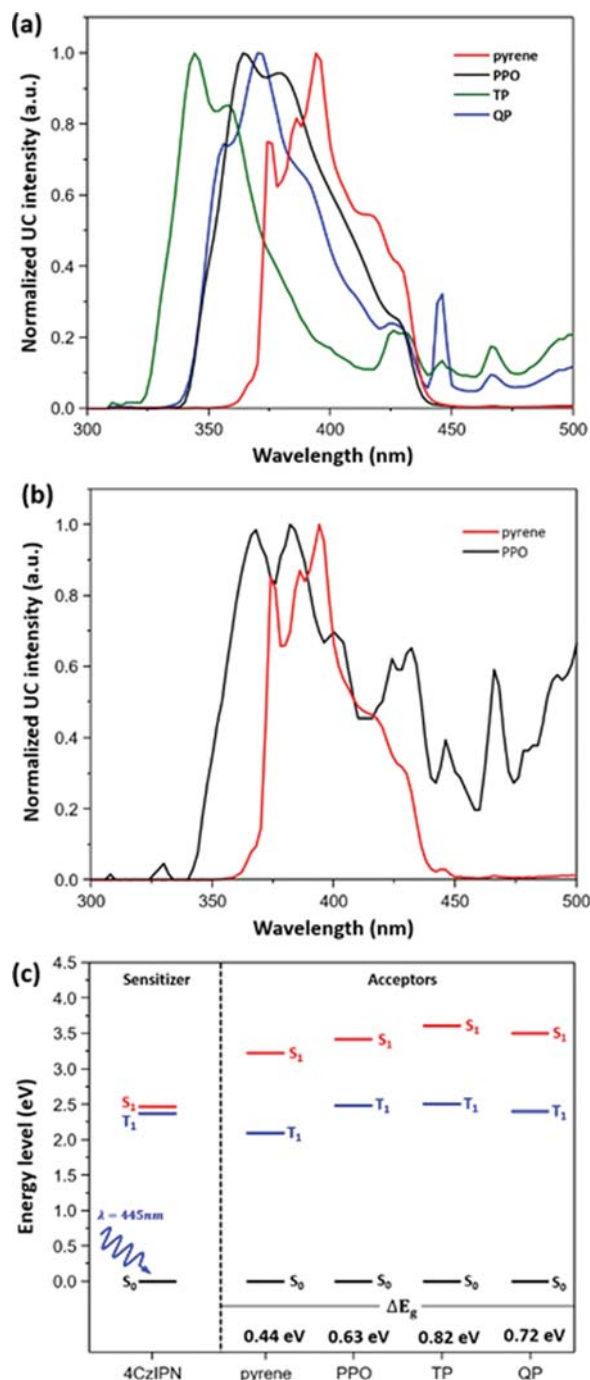

Fig. 4. Normalized UC emission spectra of 4CzIPN/pyrene, 4CzIPN/PPO, 4CzIPN/TP, and 4CzIPN/QP (a) in degassed THF and (b) in an OA/THF mixture (10 vol% OA) under 445 nm laser excitation. The UC emission spectra of 4CzIPN/TP and 4CzIPN/QP were not observed in the OA/THF mixture. (c) S_1 and T_1 energy levels of 4CzIPN, pyrene, PPO, TP, and QP, and calculated anti-Stokes shifts of 4CzIPN/pyrene, 4CzIPN/PPO, 4CzIPN/TP, and 4CzIPN/QP pairs under 445 nm laser excitation.

3. Photostability of UC Pairs

As experimentally demonstrated above, the tendency toward decreased upconverted emission with increasing laser irradiation
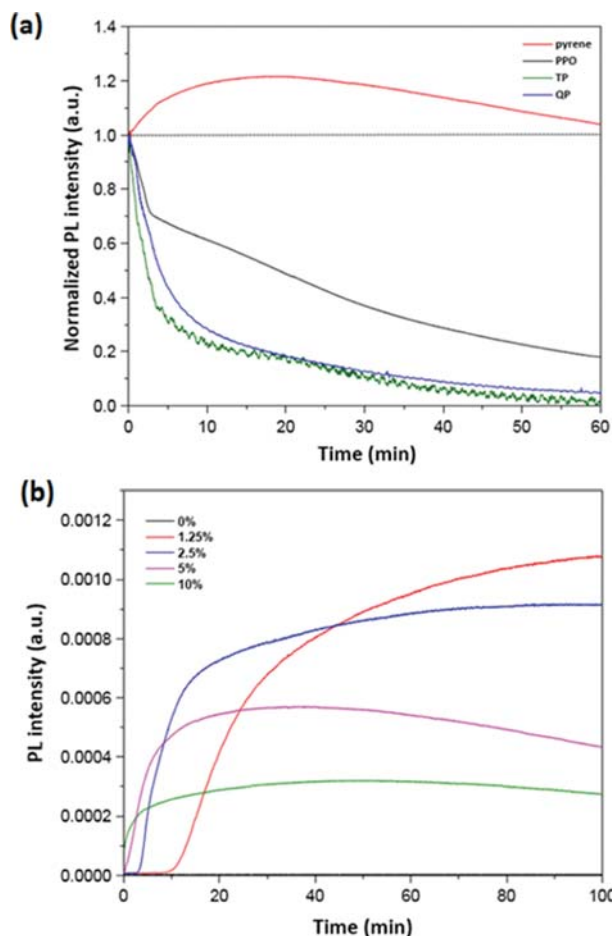
Fig. 5. (a) Photostability of UC emission from 4CzIPN/pyrene (394 nm), 4CzIPN/PPO (364 nm), 4CzIPN/TP (344 nm), and 4CzIPN/QP (370 nm) pairs in degassed THF under continuous 445 nm laser excitation. (b) Photostability of UC emission from 4CzIPN/pyrene pair (394 nm) in OA/THF mixtures with different OA concentrations under continuous 445 nm laser excitation.

Fig. 6. UC emission spectra of 4CzIPN/pyrene pair in OA/THF mixture (10 vol% OA) under continuous 445 nm laser excitation. Inset shows the corresponding UC intensity at 394 nm. The spectra were recorded every 7.5 min for 60 min.

time is attributed mainly to quenching of permeated oxygen in a typical visible-to-UV TTA-UC system [35]. However, the pyrene-based solution exhibited slightly different UC emission decay characteristics under continuous laser excitation. As shown in Fig. 5(a), the UC emission from the 4CzIPN/PPO, 4CzIPN/TP, and 4CzIPN/QP pairs decreased biexponentially over time, which is especially noticeable for the 4CzIPN/PPO pair. We confirmed that the same level of emission intensity is obtainable by adding 4CzIPN to the solutions containing 4CzIPN/PPO, 4CzIPN/TP, and 4CzIPN/QP after 30 min of laser irradiation, which demonstrates that the main cause of UC emission decay is photobleaching and photodamage of the sensitizer, 4CzIPN, which are commonly observed when organic dyes are used for optical applications. Considering that $T_1 \rightarrow S_1$ reverse ISC, which is enabled by the small ΔE_{ST} value of TADF molecules, is in competition with TTET between the sensitizer and acceptor [36], it is also possible that continuous laser excitation affects the proportions of reverse ISC and TTET, resulting in rapid photobleaching early in the laser irradiation. There-
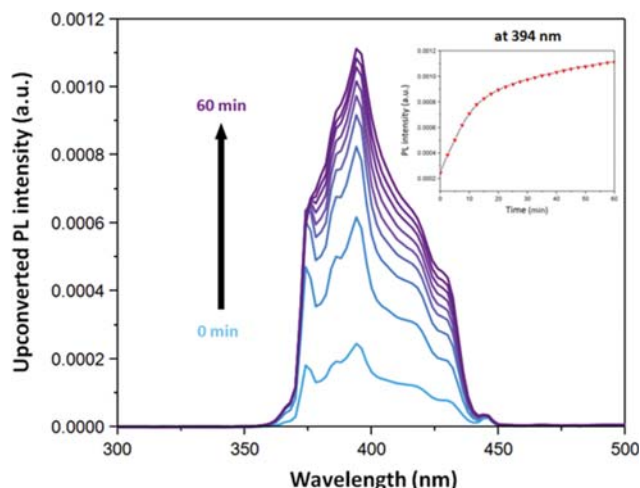
fore, it is reasonable to suggest that in the solutions containing the 4CzIPN/PPO, 4CzIPN/TP, and 4CzIPN/QP pairs, the initial exponential decay of the UC intensity can be attributed mainly to both photobleaching of 4CzIPN and the competition between reverse ISC and TTET, and the second exponential decay is due to the typical oxygen quenching behavior.

In contrast to the solutions containing the 4CzIPN/PPO, 4CzIPN/TP, and 4CzIPN/QP pairs, that containing the 4CzIPN/pyrene pair showed a significant increase in UC intensity over time in both the deaerated solution (Fig. 5(a)) and the OA/THF mixture (Fig. 5(b)). To further investigate the effect of OA concentration on the UC intensity and photostability, OA/THF mixtures containing the 4CzIPN/pyrene pair with different OA concentrations (0-10 vol%) were kept under continuous 445 nm laser excitation for an extended time. As shown in Fig. 5(b), the maximum obtainable UC intensity tends to decrease as the OA concentration increases. The decrease in UC emission is obviously attributable to the increased viscosity and relatively limited diffusion, because TTA-UC is fundamentally based on intermolecular energy transfer and thus is strongly affected by molecular diffusion. Moreover, our results indicate that inclusion of only 1.25 vol% OA in the 4CzIPN/pyrene solution facilitates efficient TTA-UC in an air-saturated environment. Further, as the OA content decreases, a relatively long excitation time is required to obtain the maximum UC intensity. It is reasonable to expect that, because the antioxidant content of OA is not sufficient to quickly reduce singlet oxygens at low OA concentration, the triplet energy of the sensitizer is quenched by oxygen early in the irradiation time. Further evidence of the increase in upconverted emission from the OA/THF mixture containing the 4CzIPN/pyrene pair is provided by measuring the UC spectra over time under continuous 445 nm laser excitation (Fig. 6). The UC intensity at 394 nm clearly increases consistently as the laser exposure time increases. In the initial stage of irradiation, the UC emission spectra show three distinct peaks at 374, 384, and 394 nm, which are consistent with pyrene fluorescence. After approximately

60 min of laser exposure time, we could not observe the peaks at 374 and 384 nm, but the peak at 394 nm still remained the highest.

4. Power Dependence and UC Quantum Yield of 4CzIPN/Pyrene Pair

To confirm that the UC emission from the 4CzIPN/pyrene pair is produced by the TTA-UC mechanism, we measured the power dependence of the UC intensity. In typical TTA-UC systems, the UC emission intensity shows quadratic and linear dependence on the incident light intensity in low and high intensity ranges, respectively [37]. Indeed, in our visible-to-UV TTA-UC system using the 4CzIPN/pyrene pair, the UC emission intensity gradually transitioned from a quadratic (slope=2.0) to a nearly linear (slope=1.1) dependence on the excitation power (Fig. 7(a)). This characteristic transition reflects the fact that under weak excitation, the dominant mechanism for depopulation of the acceptor's triplet states is pseudo-first-order decay, and thus the UC emission intensity displays a quadratic dependence on the excitation power, as expected for a bimolecular process. However, under a higher excitation power, TTA overtakes the pseudo-first-order decay, and the TTA-UC intensity becomes linearly dependent on the excitation power [38]. The transition region is observed at a relatively high power density in our TTA-UC system; however, considering that it is difficult to achieve efficient visible-to-UV TTA-UC between typical sensitizers and UV-emitting acceptors, the sensitizer/acceptor pair of 4CzIPN/pyrene can serve as a new chromophore couple for realizing an efficient, photostable visible-to-UV TTA-UC system even in an air-statured environment with limited diffusion.

The UC quantum yield of the 4CzIPN/pyrene pair was then measured as a function of excitation power using Coumarin 6 as a standard quantum counter (Fig. 7(b)). Note that TTA-UC is a bimolecular process that uses two photons to produce one higher-energy photon; thus, the theoretical maximum ϕ_{UC} value is 50% [12,39]. To avoid confusion, it is written as ϕ_{UC}' ($=2\phi_{UC}$) when the maximum yield is standardized to 100%. With increasing excitation power, the highest ϕ_{UC} value of 0.66% was obtained under our laser setup, but it did not reach the maximum achievable value. Considering that the previously reported visible-to-UV TTA-UC with a biacetyl/PPO pair in deaerated benzene showed a ϕ_{UC} value of 0.58% [17], and our ϕ_{UC} measurement was conducted using an OA/THF mixture (2.5 vol% OA) without any deoxygenation step, this value is reasonably high for visible-to-UV TTA-UC.

CONCLUSION

We demonstrated a new chromophore couple of 4CzIPN and pyrene to realize visible-to UV TTA-UC, and found that the upconverted emission from pyrene sensitized by 4CzIPN had several advantages for use in visible-to-UV TTA-UC systems, including usability in an air-saturated solution, remarkable photostability, and a relatively large UC quantum yield. Comparative analysis of the upconverted emission from four UC pairs (4CzIPN/pyrene, 4CzIPN/PPO, 4CzIPN/TP, and 4CzIPN/QP) verified the exceptional photostability of the 4CzIPN/pyrene pair. This is the first demonstration of highly photo-stable upconverted UV emission by solution-phase visible-to-UV TTA-UC in which the initial intensity is maintained even after more than an hour of continuous laser excitation in an air-saturated solution. The highest ϕ_{UC} value of the 4CzIPN/pyrene pair was measured to be 0.66% in the OA/THF mixture, which is reasonably high for visible-to-UV TTA-UC measured in an air-saturated environment with limited diffusion. Although the 4CzIPN/pyrene pair has a relatively low anti-Stokes shift, its usability in an air-saturated solution and exceptional photostability indicate its potential for use as an efficient UC pair for realizing visible-to-UV TTA-UC.
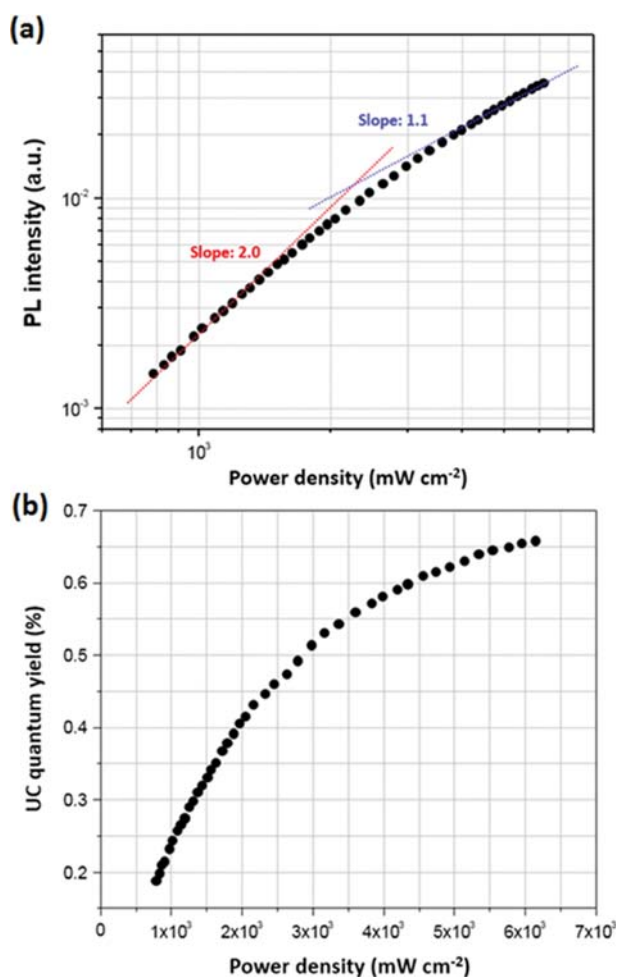
NOMENCLATURE

A : absorbance

Fig. 7. (a) UC emission intensity (394 nm) and (b) UC quantum yield of the 4CzIPN/pyrene pair in OA/THF mixture (2.5 vol% OA) as a function of excitation power density under 445 nm laser excitation.

ΔE_{ST} : energy difference between S_1 and T_1 states

I   : integrated fluorescence intensity

η : refractive index of solvent

ϕ : quantum yield

ϕ_{UC} : TTA-UC efficiency

REFERENCES

1. S. Sarina, E. R. Waclawik and H. Zhu, *Green Chem.*, **15**(7), 1814 (2013).

2. S. G. Kumar and L. G. Devi, *J. Phys. Chem. A*, **115**(46), 13211 (2011).

3. J. Chen, S. Loeb and J.-H. Kim, *Environ. Sci.: Water Res. Technol.*, **3**(2), 188 (2017).

4. T. F. Schulze and T. W. Schmidt, *Energy Environ. Sci.*, **8**(1), 103 (2015).

5. T. Trupke, M. A. Green and P. Würfel, *J. Appl. Phys.*, **92**(7), 4117 (2002).

6. Y. Y. Cheng, B. Fückel, R. W. MacQueen, T. Khoury, R. G. C. R. Clady, T. F. Schulze, N. J. Ekins-Daukes, M. J. Crossley, B. Stannowski, K. Lips and T. W. Schmidt, *Energy Environ. Sci.*, **5**(5), 6953 (2012).

7. G. Chen, J. Seo, C. Yang and P. N. Prasad, *Chem. Soc. Rev.*, **42**(21), 8304 (2013).

8. V. Gray, D. Dzebo, M. Abrahamsson, B. Albinsson and K. Moth-Poulsen, *Phys. Chem. Chem. Phys.*, **16**(22), 10345 (2014).

9. J. de Wild, A. Meijerink, J. K. Rath, W. G. J. H. M. van Sark and R. E. I. Schropp, *Energy Environ. Sci.*, **4**(12), 4835 (2011).

10. J.-H. Kim, F. Deng, F. N. Castellano and J.-H. Kim, *Chem. Mater.*, **24**(12), 2250 (2012).

11. Y. Y. Cheng, B. Fückel, T. Khoury, R. G. C. R. Clady, M. J. Y. Tayebjee, N. J. Ekins-Daukes, M. J. Crossley and T. W. Schmidt, *J. Phys. Chem. Lett.*, **1**(12), 1795 (2010).

12. A. Monguzzi, R. Tubino, S. Hoseinkhani, M. Campione and F. Meinardi, *Phys. Chem. Chem. Phys.*, **14**(13), 4322 (2012).

13. R. S. Khnayzer, J. Blumhoff, J. A. Harrington, A. Haefele, F. Deng and F. N. Castellano, *Chem. Commun.*, **48**(2), 209 (2012).

14. J. Zhao, S. Ji and H. Guo, *RSC Adv.*, **1**(6), 937 (2011).

15. F. N. Castellano and C. E. McCusker, *Dalton Trans.*, **44**, 17906 (2015).

16. W. Wu, J. Zhao, J. Sun and S. Guo, *J. Org. Chem.*, **77**, 5305 (2012).

17. W. Wu, X. Cui and J. Zhao, *Chem. Commun.*, **49**(79), 9009 (2013).

18. J. Zhou, Q. Liu, W. Feng, Y. Sun and F. Li, *Chem. Rev.*, **115**(1), 395 (2015).

19. S. Ji, W. Wu, W. Wu, H. Guo and J. Zhao, *Angew. Chem. Int. Ed.*, **50**, 1626 (2011).

20. S. Guo, L. Xu, K. Xu, J. Zhao, B. Küçükoz, A. Karatay, H. G. Yaglioglu, M. Hayvali and A. Elmali, *Chem. Sci.*, **6**, 3724 (2015).

21. T. N. Singh-Rachford and F. N. Castellano, *J. Phys. Chem. A*, **113**(20), 5912 (2009).

22. W. Zhao and F. N. Castellano, *J. Phys. Chem. A*, **110**(40), 11440 (2006).

23. T. C. Wu, D. N. Congreve and M. A. Baldo, *Appl. Phys. Lett.*, **107**(3), 031103 (2015).

24. H. Uoyama, K. Goushi, K. Shizu, H. Nomura and C. Adachi, *Nature*, **492**, 234 (2012).

25. N. Yanai, M. Kozue, S. Amemori, R. Kabe, C. Adachi and N. Kimizuka, *J. Mater. Chem. C*, **4**(27), 6447 (2016).

26. B. S. Kim and J. Y. Lee, *ACS Appl. Mater. Interfaces*, **6**(11), 8396 (2014).

27. Q. Liu, M. Xu, T. Yang, B. Tian, X. Zhang and F. Li, *ACS Appl. Mater. Interfaces*, **10**(12), 9883 (2018).

28. V. Gray, P. Xia, Z. Huang, E. Moses, A. Fast, D. A. Fishman, V. I. Vullev, M. Abrahamsson, K. Moth-Poulsen and M. L. Tang, *Chem. Sci.*, **8**(8), 5488 (2017).

29. A. Kretzschmar, C. Patze, S. T. Schwaebel and U. H. F. Bunz, *J. Org. Chem.*, **80**(18), 9126 (2015).

30. T. N. Singh-Rachford and F. N. Castellano, *Coord. Chem. Rev.*, **254**(21), 2560 (2010).

31. L. C. Ong, L. Y. Ang, S. Alonso and Y. Zhang, *Biomaterials*, **35**(9), 2987 (2014).

32. N. Yanai and N. Kimizuka, *Chem. Commun.*, **52**(31), 5354 (2016).

33. J.-H. Kim and J.-H. Kim, *J. Am. Chem. Soc.*, **134**(42), 17478 (2012).

34. Q. Liu, B. Yin, T. Yang, Y. Yang, Z. Shen, P. Yao and F. Li, *J. Am. Chem. Soc.*, **135**(13), 5029 (2013).

35. S. Wu, G. Han, D. J. Milliron, S. Aloni, V. Altoe, D. V. Talapin, B. E. Cohen and P. J. Schuck, *Proc. Natl. Acad. Sci. USA*, **106**(27), 10917 (2009).

36. J. Peng, X. Guo, X. Jiang, D. Zhao and Y. Ma, *Chem. Sci.*, **7**(2), 1233 (2016).

37. C. Li, C. Koenigsmann, F. Deng, A. Hagstrom, C. A. Schmuttenmaer and J.-H. Kim, *ACS Photonics*, **3**(5), 784 (2016).

38. A. L. Hagstrom, H.-L. Lee, M.-S. Lee, H.-S. Choe, J. Jung, B.-G. Park, W.-S. Han, J.-S. Ko, J.-H. Kim and J.-H. Kim, *ACS Appl. Mater. Interfaces*, **10**(10), 8985 (2018).

39. K. Okumura, K. Mase, N. Yanai and N. Kimizuka, *Chem. - Eur. J.*, **22**(23), 7721 (2016).